A NEW SEISMIC PERFORMANCE UPGRADING METHOD FOR EXISTING STEEL BRIDGES USING BRBS

Tsutomu USAMI[1]

Abstract: A new seismic performance upgrading method for existing steel bridges using buckling-restrained braces (BRBs) is presented. Contrary to the conventional practice of BRBs for retrofitting steel bridges, the proposed method is to keep using the existing bracing members without replacing and to reform them to energy-dissipating members at their sites. The present paper deals with a series of background experiments, including (1) performance tests of isolated BRBs with H-section core members and (2) performance tests of rigidly-connected plane steel truss models with bare or "BRBed" H-section diagonal bracing members. Furthermore a pseudo-dynamic test is performed to determine the demand of a prototype steel truss structure subjected to severe earthquakes.

Introduction

Recent severe earthquakes in Japan, such as the 1995 Kobe and the 2011 Tohoku earthquakes have revealed the vulnerability of some steel bridge structures accompanied by various types of damage, such as local/global buckling and brittle fractures. To alleviate such problems, numerous researches have been conducted to enhance the performance through the development of new structural configurations. On the other hand some hysteretic dampers, such as buckling-restrained braces (BRBs) and shear panel dampers (SPD), attract more attention and have been extensively investigated so as to be introduced for retrofitting steel bridges like arch, truss, cable stayed bridges (Usami *et al.* 2005, Chen *et al.* 2006, Kanaji *et al*. 2008, Chen *et al.* 2011).

Almost all the BRBs installed in Japan to retrofit steel bridges are used as "replacing" the bracing members. Instead, the method proposed in this paper is to keep using the bracing members without replacing, and to reform them to energy-dissipating members at their sites by adding and bolting some buckling-restraining plates. Following our original investigations, the idea has already been implemented for retrofitting two steel highway arch bridges in Japan, one of which is shown in Figure 1(Honjo *et al.* 2012). The present paper deals with a series of background experiments, including 1)performance tests of isolated H-section BRBs (Oda and Usami, 2010) and 2)performance tests of rigidly-connected plane steel truss models with bare H-section or "BRBed" H-section diagonal bracing members (Funayama *et al*. 2012). Furthermore a pseudo-dynamic test is performed to determine the demand of a prototype truss structure under severe earthquake. Beside the performance tests, elastic-plastic large displacement analyses are carried out to substantiate the test results.

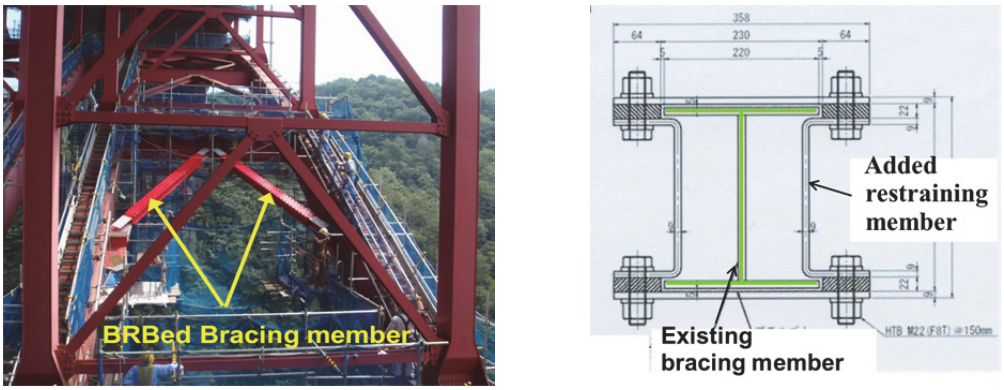

Figure 1 Arch bridge with "BRBed" bracing member (Courtesy of West NEXCO, Japan)

[1] Emeritus Professor, Nagoya University, Nagoya, Japan, usamit@meijo-u.ac.jp

Performance Tests of Isolated H-section BRBs (Oda and Usami, 2010)

Cyclic tension-compression tests of one bare H-section member and two BRBs having a core member of the same H-section have been performed. Here some findings obtained from the tests are summarized. Figure 2 shows the cross-section of the "BRBed" test specimen comprising the bare H section member and the added restraining member that are composed of two channel members bolted together with two thin cover plates. The member slenderness ratio of the bare H-section about the weak axis is 100. Gaps of 1mm are provided between the H-section flange outer surfaces and the thin cover plate inner surfaces. The observed axial force P/P_y (P_y: squash load) versus axial displacement δ/δ_y (δ_y: axial displacement corresponding to P_y) curves are shown in Figures 3 (a) and (b) for the bare and BRBed H-section members, respectively. It is seen that the remarkable amount of energy dissipation capacity can be expected in BRBed member compared with the bare member. The failure mode of the BRBed member is shown in Figure 4, where local buckling of the H-section flange plates near the specimen's end is observed. This fact indicates that, if the flange plates had been adequately restrained against local buckling, higher energy dissipation capacity would have been obtained.

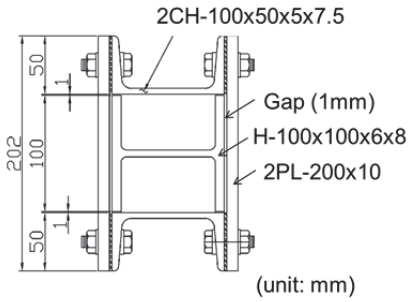

Figure 2 "BRBed" H-section test specimen (isolated BRB member test)

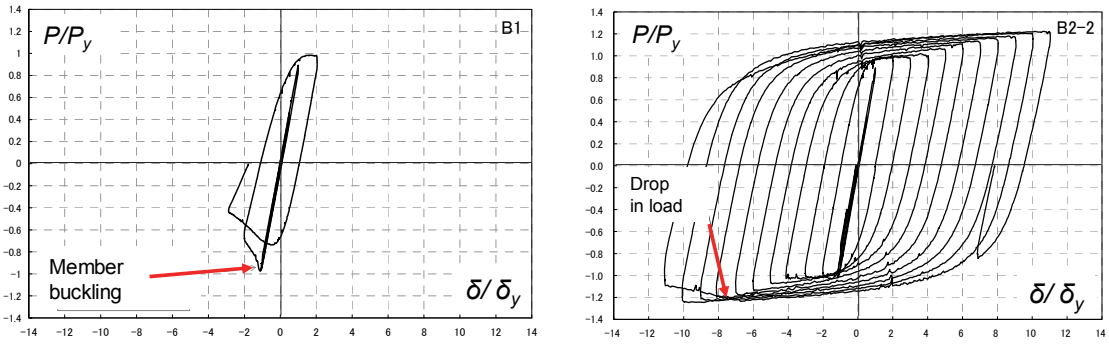

(a) Bare H-section (b) "BRBed" H-section

Figure 3 Axial force versus axial displacement curves of isolated member tests

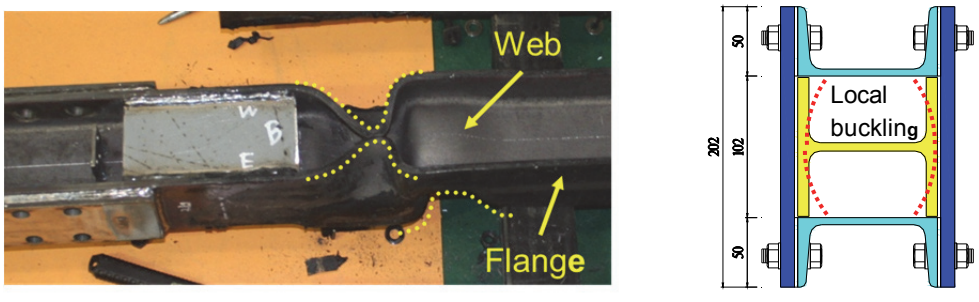

(a) H-section core member end (b) Cross-section

Figure 4 Local buckling failure mode of "BRBed" core member end

Performance Test and Analysis of Plane Steel Truss Models with and w/o BRBs

(1) Capacity Tests (Cyclic and Monotonic Loadings)

Shown in Figure 5 is the general view of the test specimen. A total of four truss specimens are tested as listed in Table 1. The dimensions are identical except for the diagonal members. The cross-section of the upper and lower chords and the vertical members is H-100×100×6×8mm made of mild steel (SS400). The bare H-section diagonal members whose cross section is H-92×50×6×4 was manufactured from H-100×100×6×8 by cutting and grinding the flanges. The specimen H-Cy was tested under cyclic loading. The core member of the "BRBed" diagonal member in specimens BRB-H-Cy & BRB-H-Mo is the same as H-Cy. The member slenderness ratio of the bare H-section diagonal member about the weak axis is 80.0. In order to effectively restrain local/global buckling of the core member, the restraining member whose cross-section comprising a pair of channels, two thin plates and four plate strips (PL-18x4.5mm) shown in Figure 5 is installed. The four plate strips welded to the channels play a role of preventing local flange buckling of the core member, the importance of which was found in the component test as stated before. The specimen BRB-H-Cy was tested under cyclic loading and BRB-H-Mo under monotonic loading.

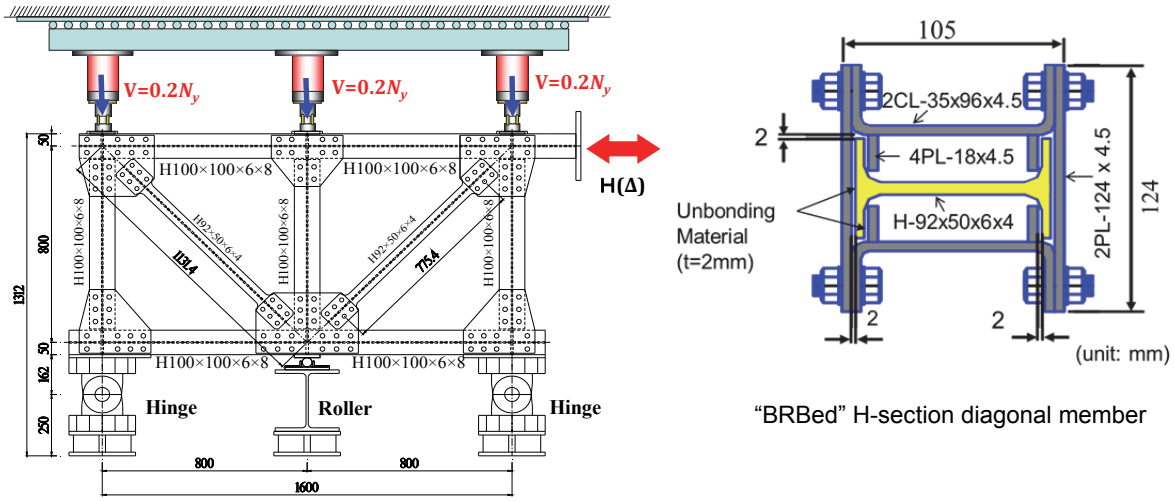

Figure 5 Configuration of truss test specimen

Table 1 Truss test loading patterns

No.	Specimen	Diagonal member	Loading Pattern	Slenderness ratio
1	H-Cy	① bare H-sectin	Cyclic	Diagonal member = 80
2	BRB-H-Mo	②BRBed H-section	Monotonic	
3	BRB-H-Cy		Cyclic	
4	BRB-H-Hy		Pseudo- dynamic	

The test specimen is vertically installed in a rigid testing frame as shown in Figure 6. The horizontal load is applied by an actuator of 1,000 kN. In order to simulate the design dead load of bridge RC decks, three constant loads of an identical magnitude, V=127kN (=0.2N_y, N_y=axial yield load of the vertical members), are applied on the top of the vertical members by three vertical actuators of 300 kN each. The vertical actuators are movable along with the movement of the specimen's top chord member during the test. The left and right bottom

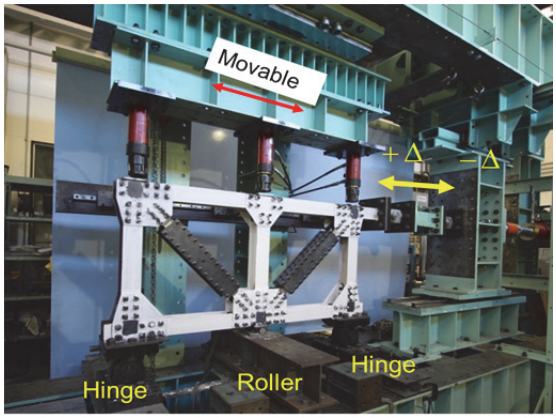

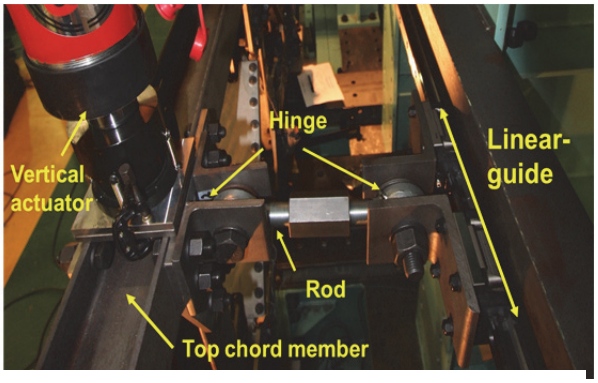

Apparatus for out-of-plane displacement constrain

Figure 6 Test set-up

Table 2 Material properties of test specimen

Member	steel	Thickness (mm)	E (GPa)	σ_y (MPa)	σ_u (MPa)	δ_u (%)	v
H-section Flange	SS400 (mild steel)	7.6	210	314	452	28.4	0.285
H-section Web		5.7	207	300	447	27.9	0.284
Gusset plate		8.0	209	289	425	27.5	0.288
BRB's restrainer		4.3	213	299	432	26.4	0.287

Note: E=Young's modulus, σ_y=yield stress, σ_u=ultimate tensile strength, δ_u=*elongation,* v=Poisson's ratio.

corner joints of the truss are hinged, and the middle bottom joint is located on a sliding support. In order to prevent the out-of-plane deformations of the test specimen, its top chord member is supported at its three joints by pin-connected bars as shown in Figure 6. One ends of the bars are connected to the test specimen and the other ends are supported by the blocks which can move along the given fixed path.

Table 2 lists the average values of the material properties measured from tension coupon tests. The slip-critical bolted connections of M16 high-strength bolts in standard size holes were used between chords or braces and gusset plates.

Figures 7(a) and (b) show comparisons of the horizontal force H versus drift Δ relationships of H-C_y and BRB-H-Cy specimens, respectively. A pushing force and the corresponding drift are taken positive (see Figure 6). In H-Cy specimen, global buckling of the right and left diagonal braces occurred at the positive and negative peak loads (points A & B), respectively, causing sudden drop in the load carrying capacity (see Figures 8). On the other hand, in BRB-H-Cy no global buckling was observed in the diagonal members. Instead, gradual drop in the loads was caused by the local damages (cracks) of bolt holes in the bottom chord members near the left and right bearings (see Figures 9). In order to compare the behavior of the test specimens, the average envelope curves are given in Figure 7(c). The failure points are defined when the load carrying capacity of the specimen is decreased by 5%. Table 3 summarizes the test results including the maximum load H_{max}, the failure drift Δ_{95}, the energy dissipation capacity ΣE (area enclosed by the hysteretic loops up to the failure point.). As shown in Figure 7(c) and Table 3, the failure drift and the dissipated energy of BRB-H-C_y are, respectively, about 2.77 and 5.85 times as large as those of the H-C_y specimen. Moreover, from the observation of these tests, the failure of the H-C_y specimen is due to the overall buckling of the diagonal braces, while the failure of the BRB-H-C_y specimen is caused by the damages to the left and right bottom corner joints. The buckling of the diagonal braces makes the specimen's load carrying capacity decrease quickly, which is obviously harmful to the bridge under strong earthquakes. The damage to the corner joints is progressive so that

the load carrying capacity of the truss does not drop clearly. Besides, the BRB-H-C_y specimen is capable of dissipating more energy than the H-C_y specimen.

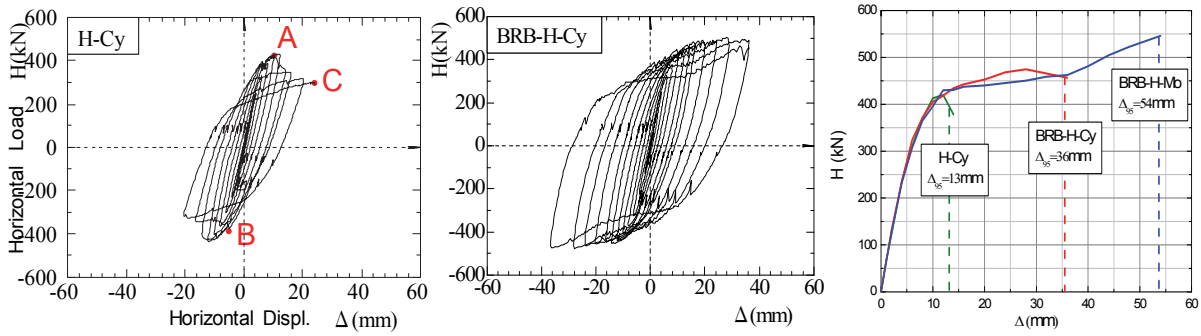

(a) Bare H (H-Cy) (b) "BRBed" H (BRB-H-Cy) (c) Envelope curves

Figure 7 Horizontal load *H* versus horizontal displacement (drift) *Δ* curves

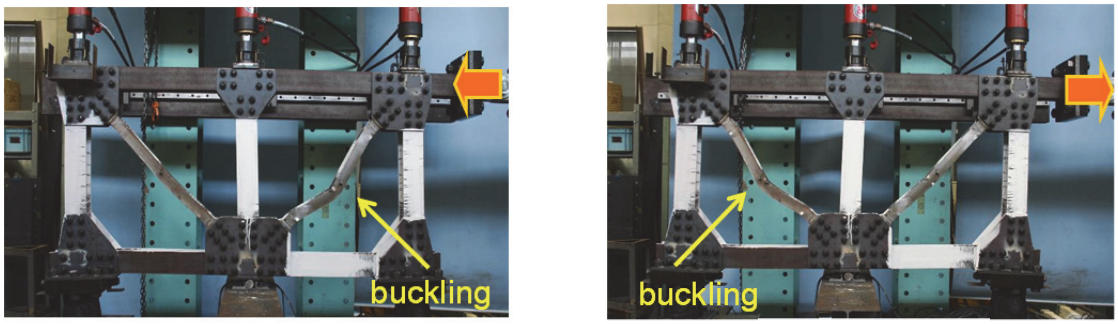

(a) Δ= +24mm (b) Δ= -24mm

Figure 8 Member buckling of H-Cy (bare H-section diagonal member)

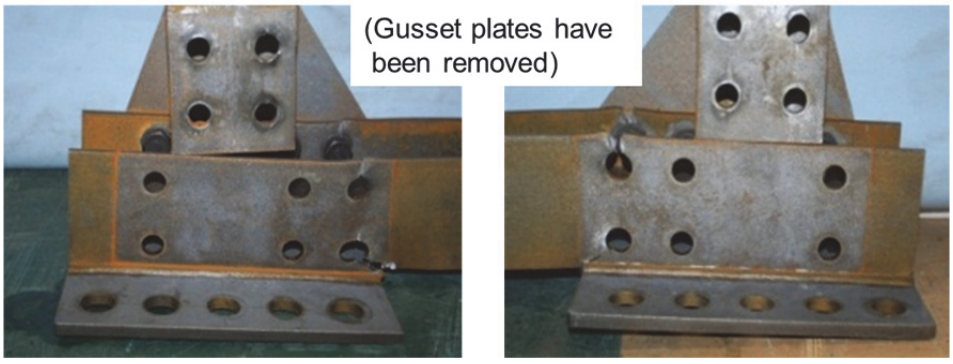

(a) Left joint (b) Right joint

Figure 9 Damage to the bolt holes of bottom corner joints (BRB-H-Cy)

Table 3 Summary of capacity test results

Specimen	H_{max} [kN]	Δ_{95} [mm]	Ratio	ΣE [kN.m]	Ratio
H-Cy	420	13.0	1	20.5	1
BRB-H-Mo	546	54.0	4.15	25.8	1.26
BRB-H-Cy	475	36.0	2.77	120	5.85

(2) Demand Test (Pseudo-dynamic Loading)

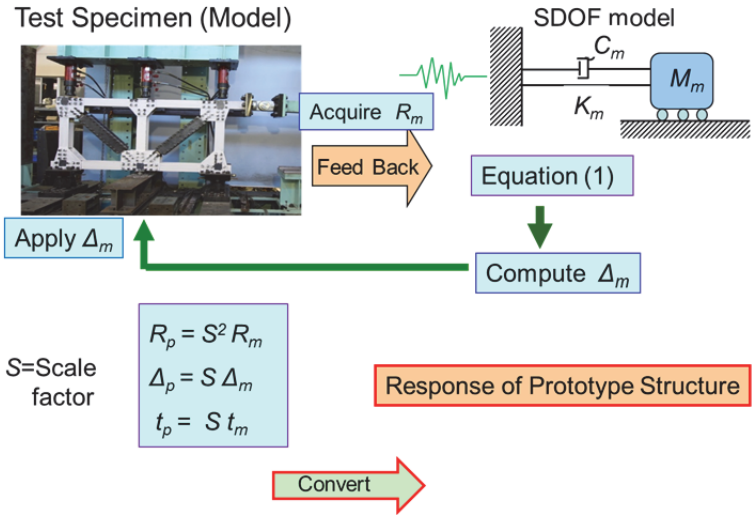

Figure 10 Pseudo-dynamic test procedure of scaled model

The pseudo-dynamic test method (PDTM) is an on-line computer controlled testing technique devoted to the determination of the demand (or responses) of a structure subjected to severe earthquakes. In this paper PDTM for scaled models developed in Nagoya University (Kumar *et al.* 1997) is used. The method is at present applicable to a single degree of freedom (SDOF) system only, but has a merit of being able to obtain seismic responses of a prototype real structure from a model test. The scheme is schematically shown in Figure 10. The truss test specimen is modelled as SDOF model with the top horizontal displacement Δ as the variable, and the sum of the vertical loads, $3V$, is converted to the equivalent mass M_m as $3V/g=39.0\times10^3$ kg, where g is the acceleration of gravity. Then it is possible to utilize the same loading device as the capacity test. Among the three procedures proposed by Kumar et al. (1997) the procedure 1B is used. In the procedure the equation of motion to be solved during the test is for the model, i.e.

$$M_m\ddot{\Delta}_m + C_m\dot{\Delta}_m + R_m = -M_m\ddot{x}_{0m} \tag{1}$$

where M_m =mass, C_m=damping coefficient=$2\xi_m\sqrt{K_m \cdot M_m}$, ξ_m=viscous damping ratio, K_m=elastic stiffness, R_m=restoring force, Δ_m=relative horizontal displacement, and $\ddot{x}_{0m}$=ground acceleration. All the quantities with suffix "m" denote the quantities related to the model, and the quantities with suffix "p" the prototype in the following. The test is carried out entirely on the model without considering the prototype. However, this requires that the input accelerogram be modified as $\ddot{x}_{0m}=S\cdot\ddot{x}_{0p}$ and $t_m=t_p/S$; i.e., the acceleration must be scaled up by S and the time scaled down by $1/S$. The response quantities obtained from the test are then converted to those corresponding to the prototype by $R_p=S^2\cdot R_m$, $\Delta_p=S\cdot\Delta_m$ and $t_p=S\cdot t_m$. The scale factor S used in the test is 10.0. The viscous damping ratio ξ_m is assumed to be 0.05 and the same value is used for the prototype. The test specimen is BRB-H-Hy in Table 1, which is identical to BRB-H-Cy. The natural period T of the prototype corresponding to the test specimen is 1.51 second. The input earthquake motion used is the one recorded during the 2011 Tohoku earthquake in the Sendai region (denoted as Sendai). The Tohoku earthquake is an interlocking type earthquake having two peculiar characteristics: long effective duration over 300 second and two PGAs (peak ground accelerations) both exceeding 1g (Figure 11). This sort of earthquake motion has never been used to check the safety of BRBs. In addition another earthquake motion called JR Takatori N-S (denoted as

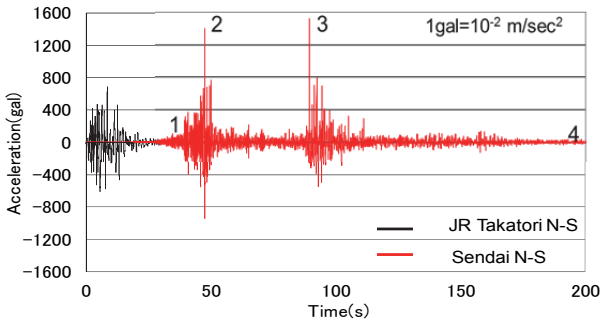

Figure 11 Input earthquake motions (Sendai N-S and JR Takatori N-S)

JR Takatori) is used for numerical analysis (Figure 11), which was recorded in 1995 Kobe earthquake and adopted after a slight modification in the current JRA bridge design code (JRA, 2012). The JR Takatori accelerogram has been frequently used in Japan to check the safety of designed bridge structures including seismic dampers because of its inherent power compared with the other seismic motions specified in JRA specification. The value of PGA of JR Takatori is 0.66g and the effective duration is about 60 second, both of which are much smaller than those of Sendai earthquake.

(3) Numerical Analysis Method (Cyclic, Pseudo-dynamic and Dynamic Loadings)

In order to substantiate the test results, elastic-plastic large displacement analyses have been carried out. The analytical methods for cyclic and dynamic loadings are essentially the same, but in the case of dynamic or pseudo-dynamic loading the three vertical loads are replaced by the equivalent masses as shown before. The main assumptions and conditions used in the analyses are as follows:

1) All the joints are rigidly connected.
2) The gusset plate thickness is added to the member flange thickness at each joint.
3) The left and right bearings are modeled using offset (rigid) elements of 210 mm in length as shown in Figure 12. Each of the bottom ends of the offset elements is pinned and the top end is rigidly connected to the bottom chord member.
4) Initial deflection is considered only for the bare H-section diagonal members (Specimen H-Cy) with the maximum value of L/1,000 (L=diagonal member length).
5) FEM beam elements are used for all the members except the BRB diagonal member in which a pin-ended truss element is used (Figure 12).
6) Bi-linear kinematic hardening rule with $E_2=E/60$ (E=elastic modulus, E_2=strain-hardening modulus) for the BRB members and $E_2=E/100$ for the other members is employed throughout.

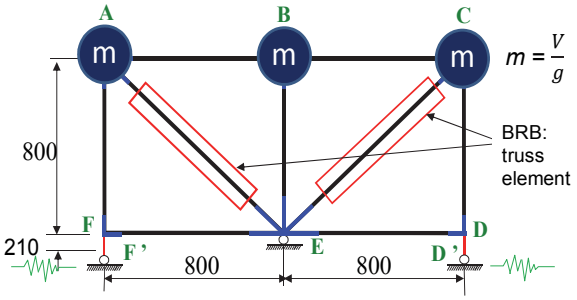

Figure 12 Numerical dynamic analysis model

(4) **Test Results with Numerical Analyses Compared**

As an example of a comparison between test and analysis under cyclic loading, Figure 13 is presented for the BRB-H-Cy test specimen. Although the loads are generally smaller in analysis, the agreement seems to be satisfactory.

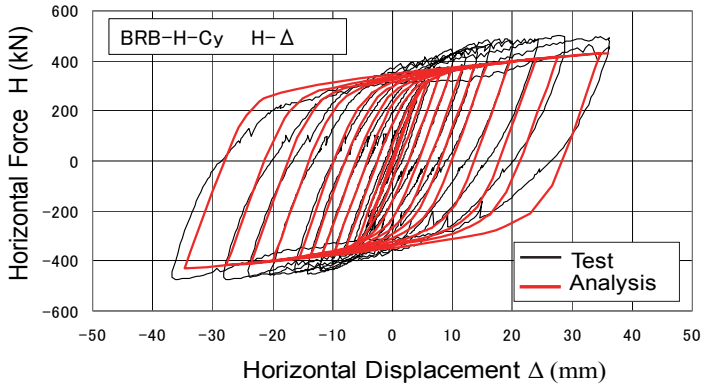

Figure 13 Comparison of cyclic test and analysis (model scale)

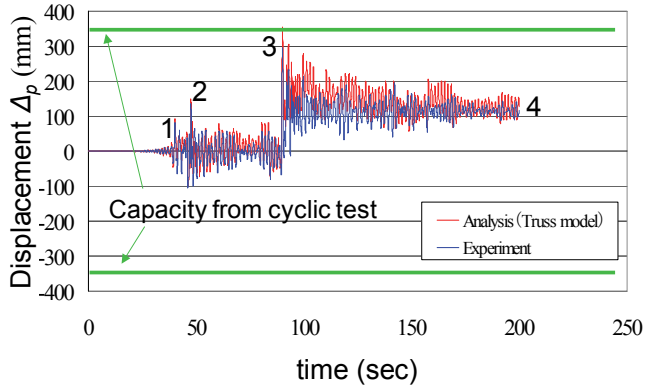

Figure 14 (a) Comparison of pseudo-dynamic test and numerical analysis
-Displacement time history (prototype scale)

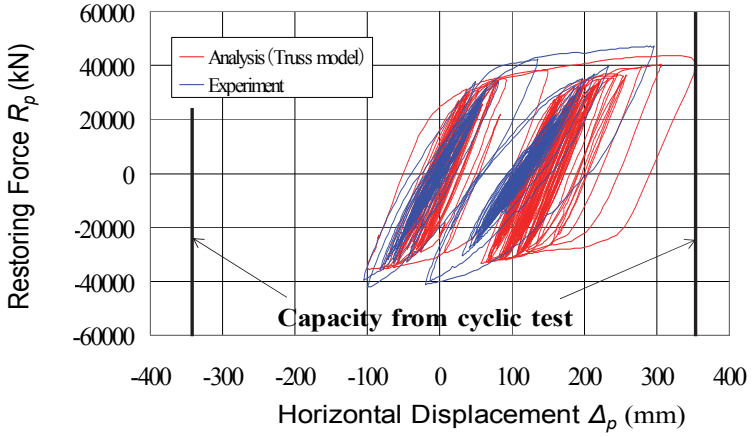

Figure 14(b) Comparison of pseudo-dynamic test and numerical analysis
-Restoring force versus displacement hysteretic relation (prototype scale)

Table 4 Comparison of pseudo-dynamic test and numerical analysis results

Earthquake	Δ_{max}/h'		Δ_R/h'		ε_{max} (%)		CID (%)	
	test	analysis	test	analysis	test	analysis	test	analysis
Sendai	1/34	1/29	1/85	1/79	2.4	1.7	13	11
JR Takatori	—	1/16	—	1/77	—	3.0	—	16

Note: Δ_{max}/h'=maximum drift, h'=10.1m (prototype scale), Δ_R/h'=residual drift, ε_{max}=maximum average strain of BRB's core member, *CID*=cumulative inelastic deformation (strain) of BRB's core member.

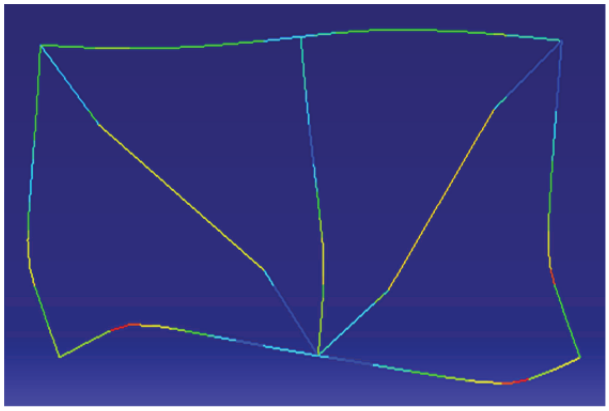

Figure 15 Residual deformations after Sendai earthquake (analysis)

Figure 14(a) and (b) show comparisons of pseudo-dynamic test (BRB-H-Hy) and numerical analysis for a) the horizontal displacement time history and b) the restoring force H versus horizontal displacement Δ hysteretic relation. All the results have been converted to those of prototype with S=10.0. In the figures a pair of horizontal and vertical lines indicate the failure drift Δ_{95} (the displacement capacity limit) obtained from the test of BRB-H-Cy. The numbers 1-4 shown in Figure 14(a) correspond to the numbers in the input earthquake motion of Figure 11. The maximum drift (Δ_{max}/h', where h' =1.01m is the total height, in model scale, of the truss including the bearing height) and the residual drift Δ_R/h' are summarized in Table 4. Shown also in Table 4 are two quantities regarding BRB's core members: the maximum value of average strains (relative axial end displacements divided by the member length), $\varepsilon_{max,}$ and the cumulative inelastic deformation (sum of inelastic components of the average strains),*CID.* The tested structure was also analysed using JR Takatori earthquake and the results are added in Table 4. From Figures 14 and Table 4, the following are observed:

1) Correlation between test and analysis is satisfactory.
2) First yielding occurs prior to the first peak of the accelerogram (point 2 in Figure 11).
3) The largest displacement Δ_{max} occurs near the second peak (point 3 in Figure 11).
4) Δ_{max} is close to but slightly smaller than the failure drift Δ_{95}.
5) The response caused by JR Takatori is larger than that caused by Sendai (Table 4).
6) Relatively large residual displacements are observed after both of the earthquakes. This is caused by severe damages occurring in the bottom chord members on the bearings as depicted in Figure 15.
7) The prototype structure considered is safe against Sendai earthquake, but unsafe against JR Takatori earthquake.

CONCLUSIONS

1）The proposed BRB system is found to be effective to prevent the progress of local and global buckling in the “BRBed” members. Thus, the seismic performance of the truss structure is enhanced significantly.
2）Damages in BRBed diagonal members are limited. However damages in the surrounding members become significant. This fact has to be seriously considered in design.
3) The demand obtained from Sendai earthquake is generally smaller than that from JR Takatori earthquake which is frequently used in Japan to check the safety of designed bridge structures with seismic dampers.
4) The proposed numerical analysis can predict the cyclic as well as dynamic behavior of the tested trusses.

REFERENCES

Kumar S, Itoh Y, Saizuka K and Usami T (1997) *Pseudo-dynamic Testing of Scaled Models,* Journal of Structural Engineering, ASCE, Vol.123, No.4, April, pp.524-526.

Usami T., Lu Z.H. and Ge H.B. (2005) *A seismic upgrading method for steel arch bridges using buckling-restrained braces*, Earthquake Engineering & Structural Dynamics, Vol.34, pp.471-496.

Chen, ZY, Ge, HB. and Usami T.(2006) *Hysteretic model of stiffened shear panel dampers*, Journal Structural Engineering, ASCE, Vol.132, No.3, pp.478-483.

Kanaji H, Fujino Y. and Watanabe E.(2008) *Performance-Based Seismic Retrofit Design of a Long-Span Truss Bridge -Minato Bridge - Using New Control Technologies,* Structural Engineering International, IABSE, Vol.18, No.3, pp. 271-277.

Oda,H and Usami T (2010) *Fabricating Buckling-restrained Braces from Existing Bracing Members-Experimental Study*, Journal of Structural Engineering, JSCE, Vol.56A, pp.499-510.

Chen XQ, Ge HB and Usami T (2011) *Seismic demand of buckling-restrained braces installed in steel arch bridges under repeated earthquakes*, Journal of Earthquake and Tsunami, Vol.5, pp.119-150.

Funayama J, Usami T, Wang CL (2012) Seismic *Upgrading Effect of Steel Truss Structures with H-section BRBs,* Structural Eng./Earthquake Eng., JSCE, Vol.68, No.4, pp.730-747.

Honjo K, Nakano M, Tasaki K, Yamazaki T, Fujii K and Otsuka H(2012) *Study on Seismic Ductility Improvement for Existing Member of Steel Bridge*, Structural Eng./Earthquake Eng., JSCE, Vol.68, No.3, pp.655-672.

JRA (2012): *Specification for Highway Bridges, Part V Seismic Design*, Japan Road Association